Supplementary Information

Self-supported nanostructured iridium-based networks as highly active electrocatalysts for oxygen evolution in acidic media

Anders Westergaard Jensen,[a] Gustav W. Sievers,[b] Kim D. Jensen,[a] Jonathan Quinson,[a] José Alejandro Arminio-Ravelo,[a] Volker Brüser,[b] Matthias Arenz,[c] María Escudero-Escribano[a]*

[a]Nano-Science Center, Department of Chemistry, University of Copenhagen, Universitetsparken 5, DK-2100 Copenhagen Ø, Denmark

[b]Leibniz Institute for Plasma Science and Technology, Felix-Hausdorff-Strasse 2, 17489 Greifswald, Germany

[c]Department of Chemistry and Biochemistry, University of Bern, Freiestrasse 3, CH-3012 Bern, Switzerland

*Corresponding author: maria.escudero@chem.ku.dk

Sample preparation

Substrate preparation:

Glassy carbon (GC) electrodes (5mm diameter, HTW, Germany) were polished and ultrasonically cleaned in acetone, isopropanol, ethanol and ultrapure H_2O (resistivity > 18.2 MΩ cm, total organic carbon (TOC) < 3 ppb, Merck Millipore). The electrodes were thereafter transferred to a vacuum chamber and for 3 min plasma-activated at a pressure of 20 Pa in an O_2 atmosphere and a radio frequency (RF) power of 300 W in order to roughen the surface and to increase adhesion. Samples were then transferred to the deposition chamber (Neoplas GmbH, Germany). To prepare the IrCo templates, the reactor chamber was evacuated to a base pressure of $5 \cdot 10^{-3}$ Pa. An argon plasma was ignited in the chamber at a working pressure of 5 Pa. First a 15 nm Ti (99.9% Mateck GmbH, Germany) interlayer was deposited onto the glassy carbon by magnetron sputtering. For the electrochemical tested samples, in addition to the Ti coating, a thin film of 100 nm Au (99.95%, Mateck) was deposited at a RF power of 50 W to ensure good adhesion for Ir deposition and avoid corrosion of the GC electrode.[1,2]

Preparation of Ir-network:

For the Ir_xCo_y film deposition, two magnetrons were equipped with planar targets of Co (99.95%, Evotec GmbH, Germany) and Ir (99.95%, MaTecK, Germany). They were located at the superior part of the recipient. The RF generators (Advanced Energy) had a driving frequency of 13.56 MHz. The recipient was configured in a way that the substrate holder is turned automatically towards the respective magnetron with the sputtering being initiated when the sample is in position below the magnetron. The RF power was chosen as 100 W for Co and 25 W for Ir. The alternating sputtering process was repeated 11 times so that the total Ir loading of the as deposited electrode was 10 μg_{Ir} cm^{-2} as measured by mass gravimetry. The atomic ratios Ir:Co were 120, 80 and 55 or $Ir_{0.8}Co_{99.2}$, $Ir_{1.2}Co_{98.7}$ and $Ir_{1.7}Co_{98.2}$, respectively.

After the sputtering, the samples were inserted in 0.1 M $HClO_4$, immediately after which Co started to dissolve. In order to accelerate the leaching and ensure a high degree of Co displacement, the samples were cycled between 0.025 V_{RHE} and 0.5 V_{RHE} at a scan rate of 100 mV s^{-1} for 50 cycles (see electrochemical section for details).

In the first scan, a broad oxidation peak was observed at 0.2 V_{RHE}, corresponding to the leaching of Co. From the 2nd to the 10th-20th scan, the hydrogen underpotential deposition (H_{upd}) region slightly decreased, indicating that some Ir is lost during the leaching protocol.

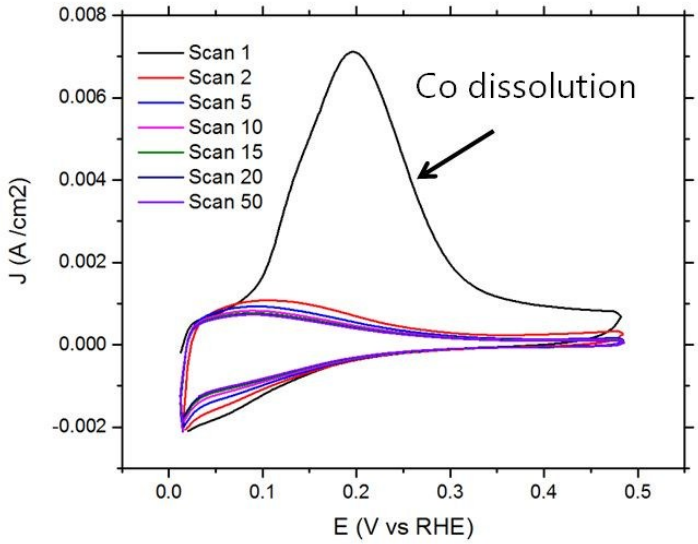

Figure S1 Electrochemical leaching of Co in Ar saturated 0.1 M $HClO_4$ of Ir-network (1:80), 100 mV s^{-1}, 0.025-0.50 V_{RHE} , represented here is the selected voltammograms of the first 50 cycles.

Preparation of Ir-black electrodes:

The ink was prepared based on the most common composition for Ir based nanoparticles (NPs) reported in the literature.[3,4] The commercial Ir NPs (Ir black, Premetek co., P40V010) were weighted and dispersed in the solution (1:3 solution of isopropanol:H_2O) along with 0.02 wt. % Nafion at a nominal concentration of 0.2 mg Ir mL^{-1}. The suspension was sonicated in an ice bath for 15 min before use.

Glassy carbon electrodes were cleaned and polished as described above, 10 µL of the catalyst ink was dropped on the glassy carbon tip. The tip was rotated at 700 rpm for 5 min to improve the distribution of the NPs afterwards it was slowly dried in a saturated isopropanol atmosphere.[5,6]

Preparation of Polycrystalline Ir electrode:

The polycrystalline Ir electrode (MaTecK, 99.995%, 5 mm diameter) was prepared by polishing the Ir electrode with 1, 0.3 and finally 0.05 µm alumina polishing suspensions (Struers) mixed with ultrapure water on a soft polishing cloth. After polishing, the electrode was rinsed and sonicated for 15 min in acetone (technical grade, Kautex), isopropanol (technical grade, VWR chemicals), ethanol (absolute ethanol, VWR chemicals) and ultrapure water.

Material Characterization

Transmission electron microscopy (TEM):

A JEOL 2100 microscope operated at 200 kV was used for transmission electron microscopy (TEM). The TEM grids were prepared by dropping solutions of Ir-network nanostructures re-dispersed in isopropanol on Cu 300 mesh grids (Quantifoil). The catalyst material was scratched from the glassy carbon substrate and re-dispersed in isopropanol (IPA, technical grade, VWR chemicals) before dropcasting. All samples were characterized by taking images of at least three different magnifications in at least five different areas of the TEM grids. ImageJ software was used to measure the size of the pores and nanostructures.

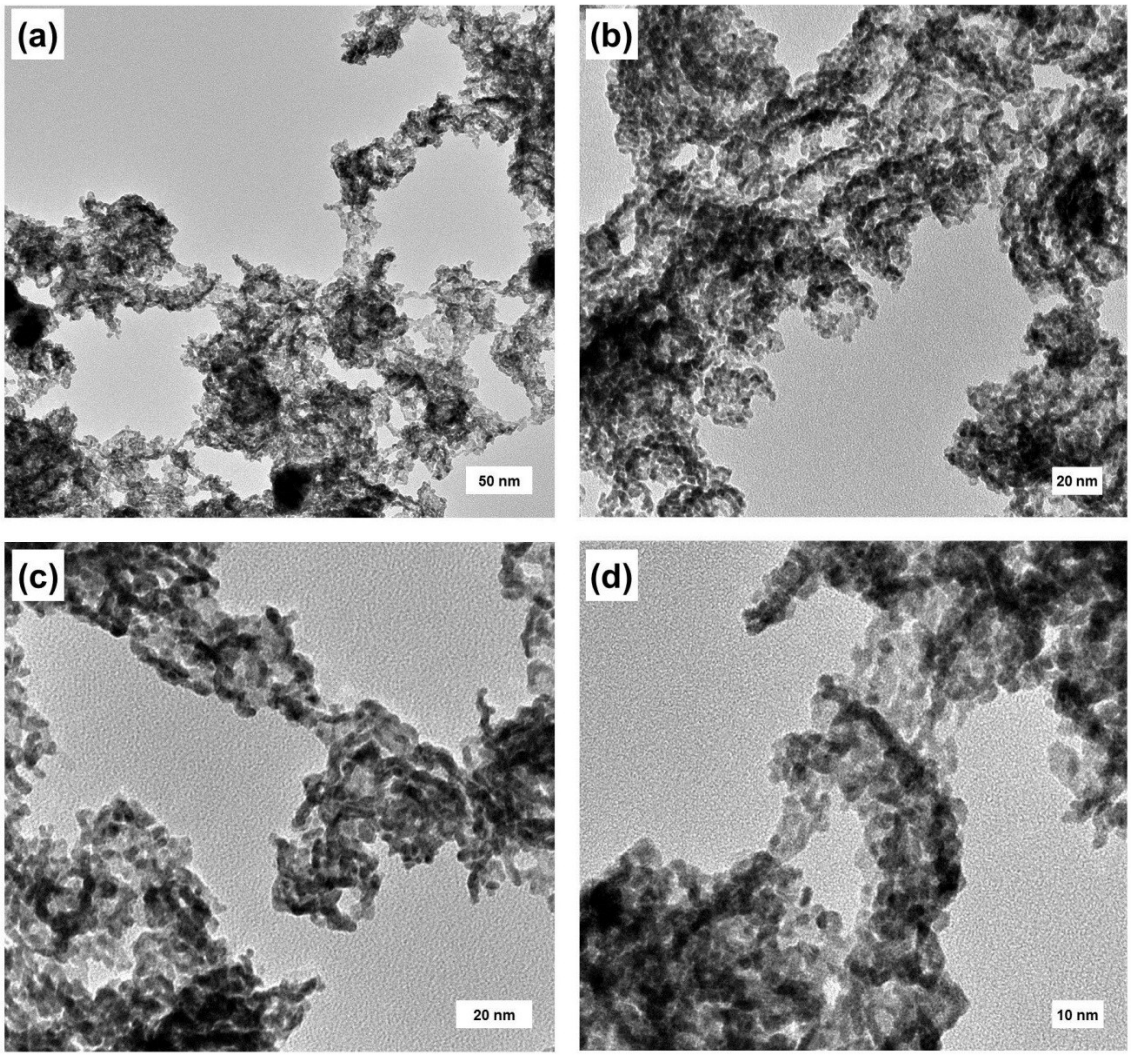

Figure S2 Representative TEM micrographs for Ir-network (1:55) at four different spots and magnifications after OER measurements.

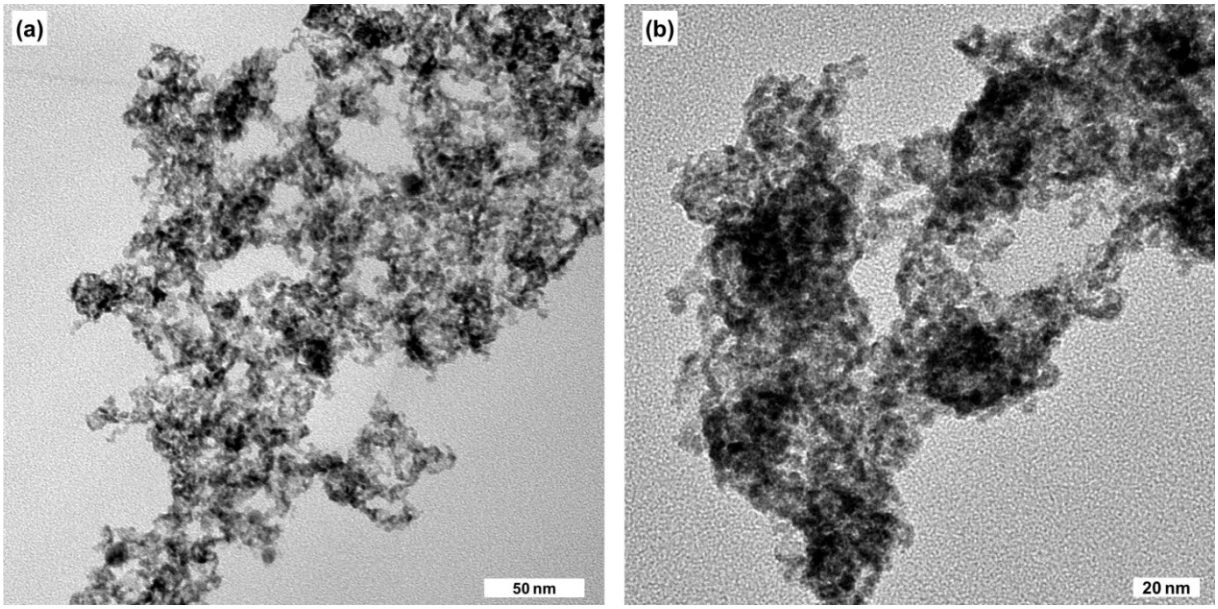

Figure S3 Representative TEM micrographs for IrO_x-network (1:55) after extended stability test @ 1.6 V_{RHE} for 12 hours.

Scanning electron microscopy (SEM):

The morphology of the sputtered Ir-network was investigated by scanning electron microscopy (JSM 7500F, JEOL, Tokyo, Japan) with a field-emission gun, a semi-in-lens conical objective lens and a secondary electron in-lens detector for high-resolution and high-quality image observation of structural features of the deposited films at a maximum specified resolution of 1.0 nm at 15 keV. The technique enables imaging the surface without any preparative coatings. The GC electrodes with and without the gold interlayer were directly placed onto the SEM unit holder.

SEM measurements were performed at least at three different magnifications (50k, 100k and 200k) at three different locations. EDS measurements were done at 15 kV at three different locations of the template sample giving the atomic compositions $Ir_{0.8}Co_{99.2}$, $Ir_{1.2}Co_{98.7}$ and $Ir_{1.7}Co_{98.2}$ respectively.

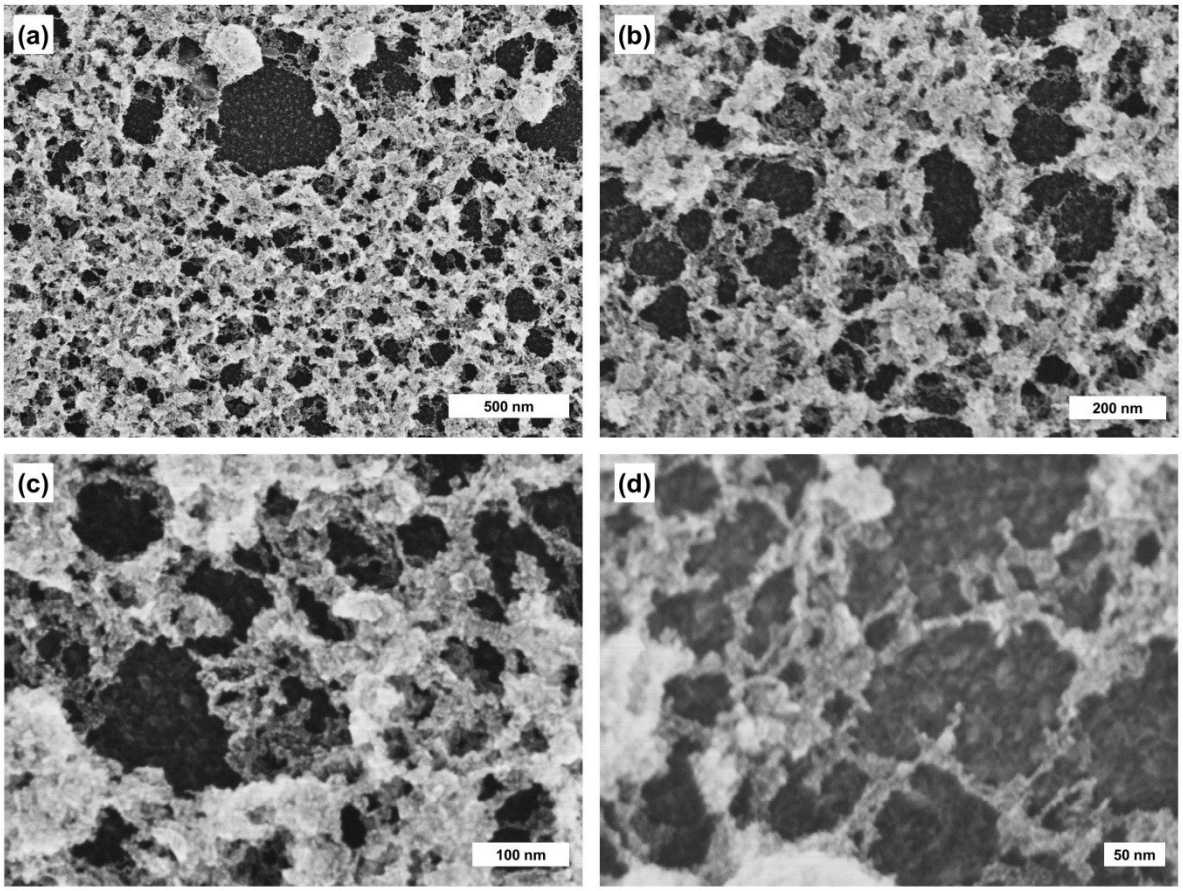

Figure S4 Representative SEM micrographs for Ir-network (1:55) after leaching, displaying the extended meso and macroporous structure on bare glassy carbon for improved contrast, at four different spots and magnifications.

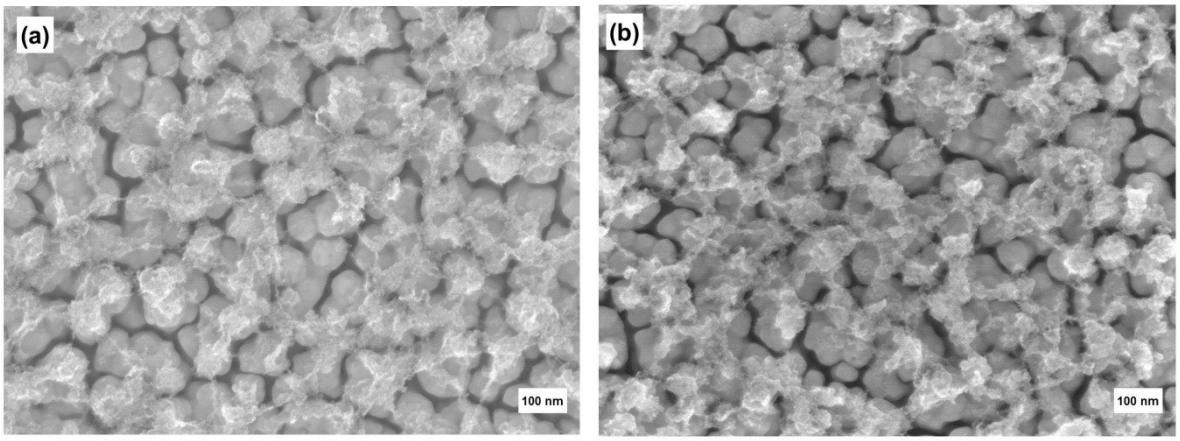

Figure S5 SEM micrographs of Ir-network (1:80) with Au substrate (a) before and (b) after OER measurements.

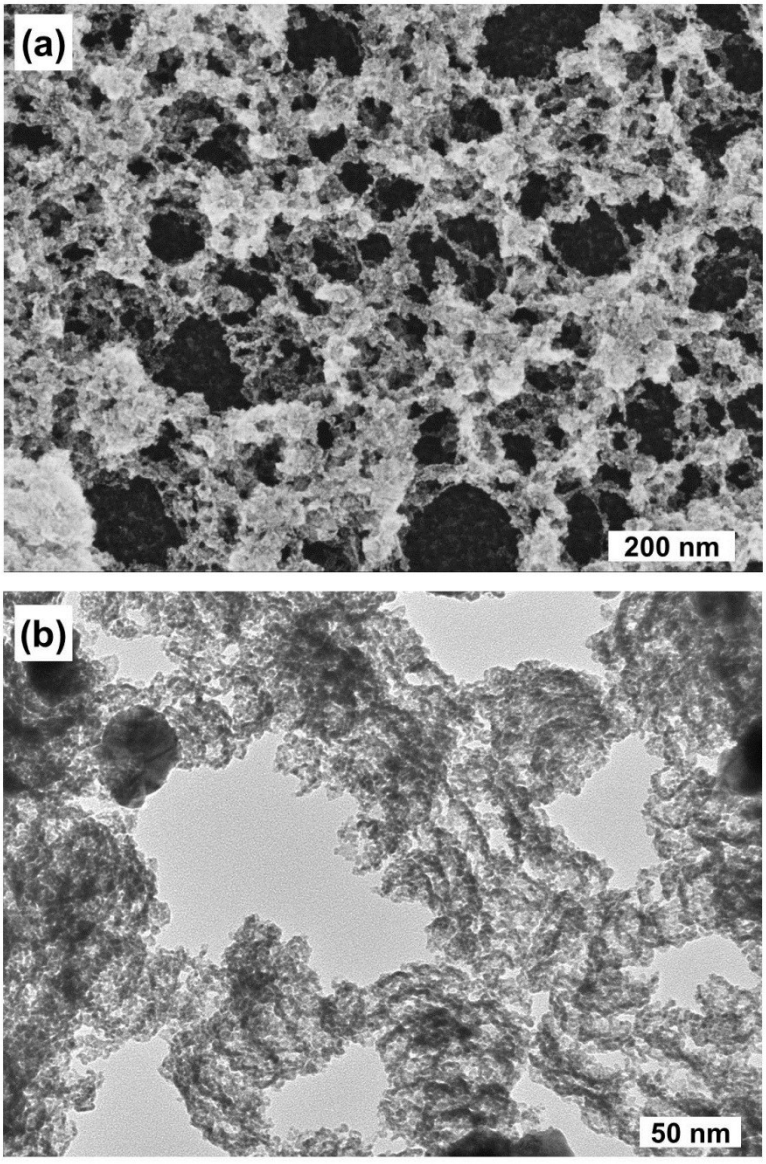

Figure S6 (a) SEM and **(b)** TEM micrographs displaying the meso/macroporous structure with a typical size of 30-150 nm.

X-ray photoelectron spectroscopy (XPS):

All XPS measurements were conducted using a Theta Probe instrument (Thermo Scientific) utilizing an Al source with an excitation energy of $E_{\gamma,Al\text{-}K\alpha}$ =1486.6 eV. The XPS chamber's base pressure was between 8.0×10^{-9} and 5.0×10^{-10} mbar. Please note that sample tilting was not applied, the X-ray beam size was 400 µm and the pass energy utilized was 100 eV. Figure S7 shows the normalized Ir4*f*, Au4*f*, Co2*p*, O1*s* and C1*s* peaks of samples as-prepared (with thick Co surface layer), after electrochemical test and after the accelerated stability test described above.

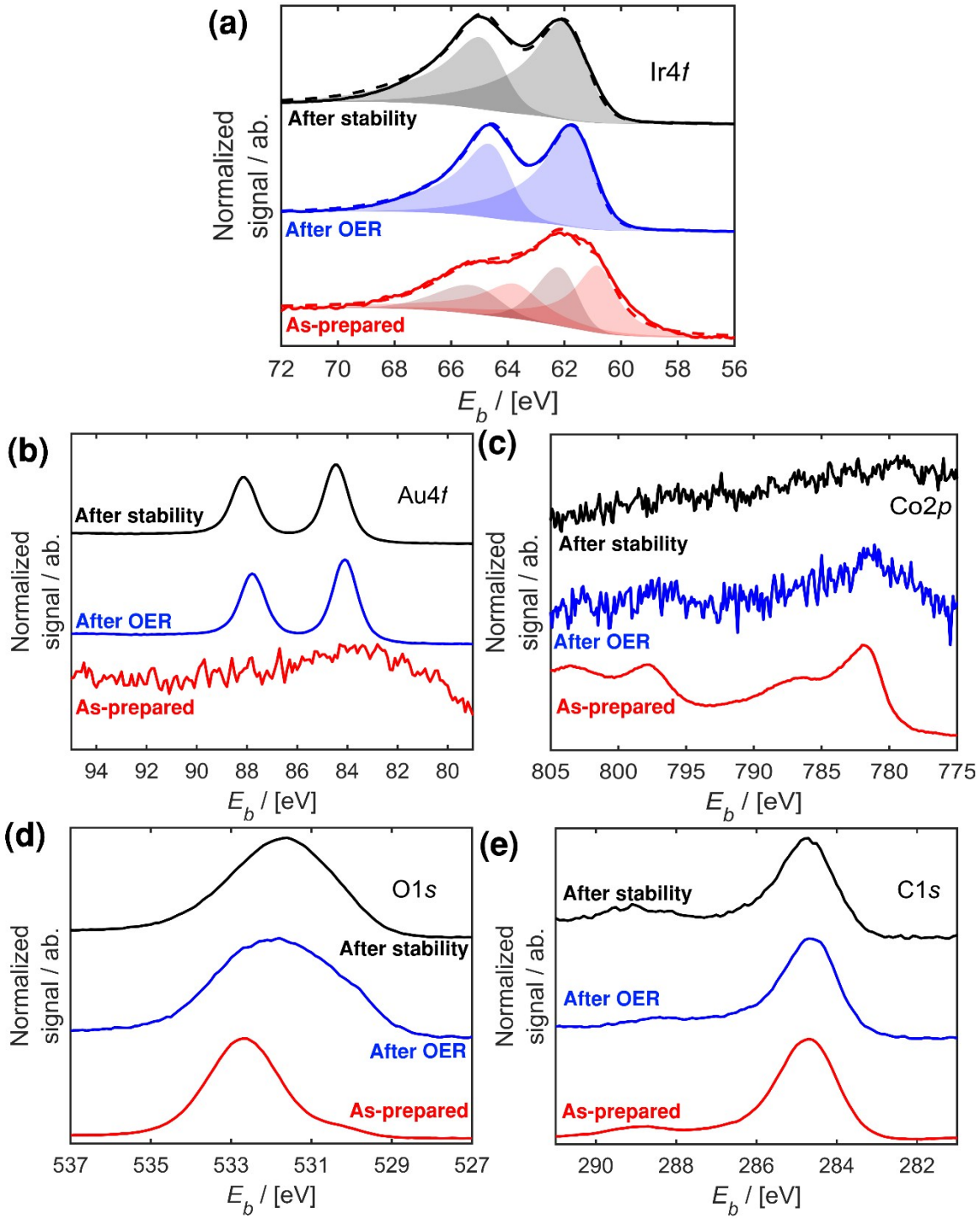

Figure S7 XPS peaks of Ir-Co thin film samples as-prepared (red), after OER testing (blue) and after extended stability test (black). **(a)** Ir4*f* peak with fitting using CasaXPS software. **(b)** Au4*f* peak. **(c)** Co2*p* peak. **(d)** O1*s* peak. **(e)** C1*s* peak. Note all peak signals (*I*) have been normalized (by [*I*-min(*I*)]/[max(*I*)-min(*I*)]), in an attempt to make differences in peak shape and position more clear.

All fitting of Ir4*f* peaks has been contingent of the constraints from the setup, the elemental doublet separation (2.95 eV)[12] and peak intensity ratios between the 7/2 and 5/2 peaks (4:3). Moreover, the full width at half maximum (FWHM) values of the peaks should be less than 2.5 eV, hereby accounting for FWHM smearing from the detector (~1 eV), sample element (0.8-1.0 eV) and X-ray source (~0.85 eV). Additionally, it should be noted that we have minimized the number of peaks to avoid overfitting; however, this approach may exclude possible satellites or exclude chemical states of the sample element.

Table S1 Atomic percentages of the XPS data from peak analysis of data depicted in Figure S7. Note values are derived from the raw XPS data using a *Shirley* type background subtraction.

Sample	Ir4*f*	Au4*f*	Co2*p*	C1*s*	O1*s*
As-prepared	1.82	0.06	8.15	47.84	42.14
After OER	13.84	22.60	0.35	42.52	20.70
After stability	22.10	8.06	0.17	25.06	44.62

The Ir4*f* peak (see Figure S7a) has been plotted as proposed by both *Schlögl and co-workers* and *Morgan and co-workers*.[13,14] The Ir4$f_{7/2}$ and Ir4$f_{5/2}$ binding energies were 61.80 and 64.75 eV, respectively, for the samples measured after OER testing. Similarly, the Ir4f peaks after stability test were 62.05 and 65.00 eV for the 7/2 and 5/2 peaks, respectively. This small change of ~0.2 eV in Ir4*f* binding energies before and after AST may arise from increased population of interstitial missing Ir[13] or due to transitions from anhydrous IrO_2 to hydrous IrO_2.[14] We must note that the Ir4*f* peak of the as-prepared sample was quite low due to the thick coverage of the protective Co layer, hence analysis was challenging. The Ir4$f_{7/2}$ and Ir4$f_{5/2}$ fitting of the as-prepared sample required two chemical states with asymmetric peak shapes.[13,14] The first coincided with Ir4$f_{7/2}$ and Ir4$f_{5/2}$ peaks at 60.80 and 63.75 eV, corresponding to metallic Ir. Besides the doublets accounting for metallic Ir4*f*, a peak with the main binding value at 62.30 eV was identified (the 5/2 peak binding was thus 65.25 eV). This second peak has previously been assigned to hydrated IrO_2[14] or Ir in a lower oxidation state than the Ir^{+4} associated with IrO_2, *i.e.* Ir^{+3}.[13,15]

From the XPS data in Figure S7b-e, one notices the following: *i*) The Au4*f* peak on Figure S7b is not observable prior electrochemical testing, suggesting complete coverage of the samples with Ir and Co. After electrochemistry, an Au signal is detected as one would expect given the porous nature of the IrO_x-network, seen in Figure S5. *ii*) The Co2*p* peak nearly disappears after electrochemistry, suggesting a pure IrO_2 phase. After stability, the Co2*p* peak is no longer identifiable. *iii*) After electrochemistry, the O1*s* peak in Figure S7d is shifted to slightly more metallic states, as one would expect from the formation of IrO_2. *iv*) The C1*s* peak of Figure S7e attains the value of 284.7 eV[16] as one would expect from advantageously adsorbed carbon.[12]

Electrochemical Characterization

Electrochemical setup:

Electrochemical experiments were performed in a three-compartment glass cell using a rotating disk electrode (RDE, Radiometer) with a 5 mm glassy carbon disk, and a potentiostat (NordicElectrochemistry) at room temperature. A Pt wire with a Pt mesh (>99.95%, Junker Edelmetalle) and a Pt RHE electrode (custom-made, Pt >99.95%, Junker Edelmetalle) were used as counter electrode and reference electrode, respectively. Prior to and after each experiment the reference electrode were checked against the reversible hydrogen potential (RHE) by bubbling H_2 (N5, 99.999%, Air Liquid) and recording cycle voltammograms with a polycrystalline Pt working electrode (Junker Edelmetalle, 99.99%, 3 mm disc).

All measurements on Ir-network and Ir-black catalysts were carried out in Ar-saturated (N5, 99.999 %, Air Liquid) 0.1 M $HClO_4$ and repeated on three catalyst films for each catalyst. The electrolytes were prepared from

deionized ultrapure water (resistivity > 18.2 MΩ cm, total organic carbon (TOC) < 3 ppb, Merck Millipore) and ultrapure concentrated $HClO_4$ (70%, Suprapur, Merck). During all measurements, the resistance between the working and reference electrode (~22-25 Ω) was determined using an AC signal (5 kHz, 5 mV) and thereafter compensated by using analogue positive feedback scheme of the potentiostat. The resulting effective solution resistance was 3 Ω or less for each experiment.

Determination of the electrochemically active surface area of pre-oxidized Ir-catalyst:

At present, there is no consensus on an experimental measure for the electrochemically active surface area of IrO_x. Several methods have been suggested including Brunauer–Emmett–Teller (BET) [7], capacitance[8], Ir^{3+}/ Ir^{4+} redox sites[4] and mercury$_{upd}$.[9] For this study, we limited the surface area estimation to ECSA before oxidation using the charge from the H_{upd} region. For Ir nanoparticles, it was recently shown that the ECSA with H_{upd} and CO-stripping before oxidation was nearly identical with the values obtained from Hg_{upd} both before and after oxidation.[10] The ECSA was estimated by integrating the hydrogen desorption charge from cyclic voltammograms (CVs) recorded between 0.025-0.80 V_{RHE}, prior to the activation step. For the calculation, a Coulombic charge of 179 µC cm_{Ir}^{-2} has been assumed.[11]

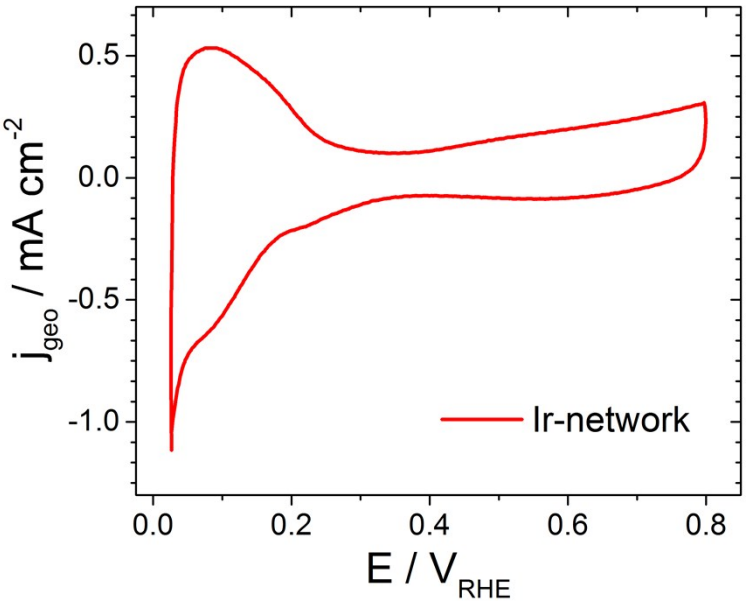

Figure S8 Typical cyclic voltammogram of the as-prepared Ir-network (1:55) after electrochemical leaching in Ar-saturated 0.1 M $HClO_4$ recorded between 0.025-0.80 V_{RHE} at a scan rate of 50 mV s^{-1}.

Determination of OER activity:

Prior to the determination of the OER activity, all catalysts (Ir-network, polycrystalline Ir and Ir-black nanoparticles) were electrochemically oxidized using a conditioning step where the catalyst was cycled from 1.2-1.8 V_{RHE} at a scan rate of 20 mV s^{-1} under a rotation rate of 3000 rpm for 20 cycles. Afterwards, the electrocatalytic activities were evaluated by linear sweep voltammetry (LSV, anodic scan) from 1.20-1.65 V_{RHE} using a scan-rate of 20 mV s^{-1} and a rotation rate of 3000 rpm. The reported activity values and Tafel analysis are based on a minimum of three separate measurements for both commercial Ir-black and Ir-network with different compositions. To ensure that the high activity was not an effect of the scan rate, we tested a IrO_x-network sample at lower scan-rates of 5 mV s^{-1} and 10 mV s^{-1} with only a minimal loss in activity.

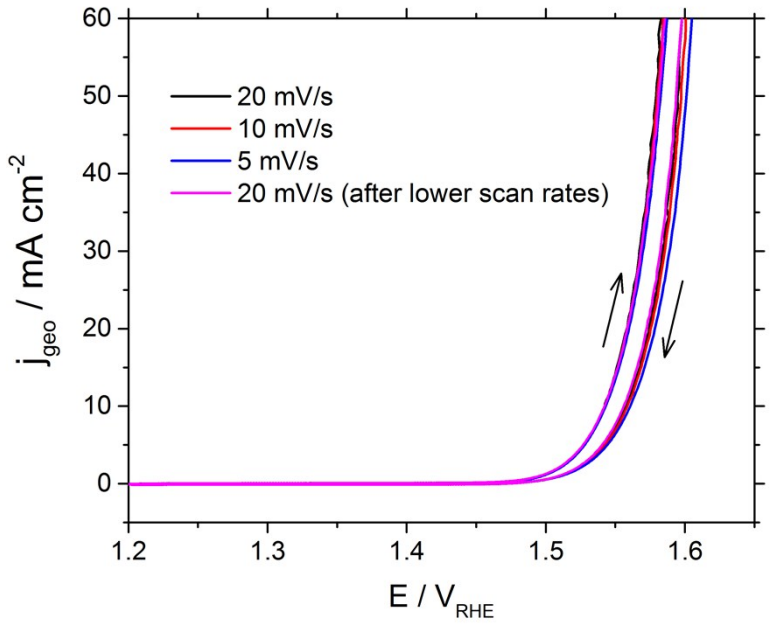

Figure S9 Cyclic voltammograms of IrO_x-network (1:80) after electrochemical oxidation in Ar-saturated 0.1 M $HClO_4$ recorded between 1.2-1.65 V_{RHE} at scan rates of 20 mV s^{-1}, 10 mV s^{-1}, 5 mV s^{-1} and 20 mV s^{-1} again after measurements at lower scan rates

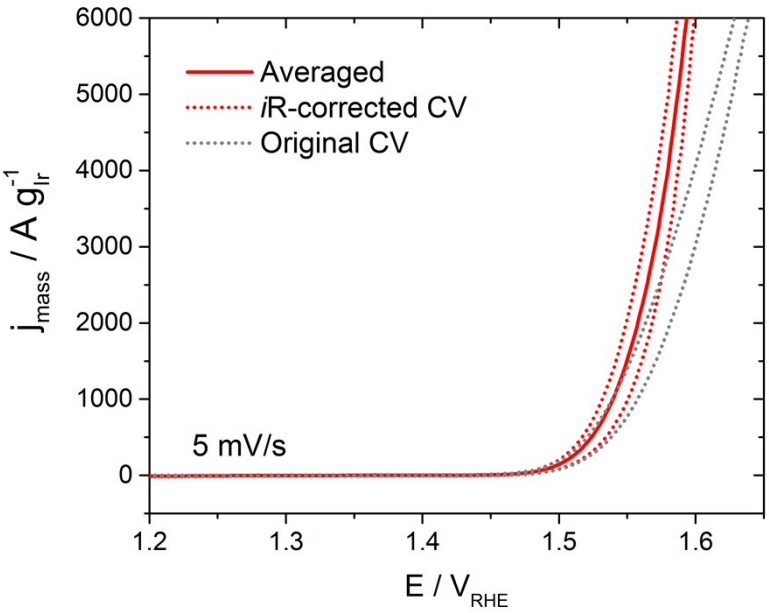

Figure S10 The measured CV of IrO_x-network (1:55) in Ar-saturated 0.1 M $HClO_4$ at 5 mV s^{-1} between 1.2-1.65 V_{RHE}, the corresponding *iR*-corrected CV and the background corrected polarization curve (average of the anodic and cathodic scan).

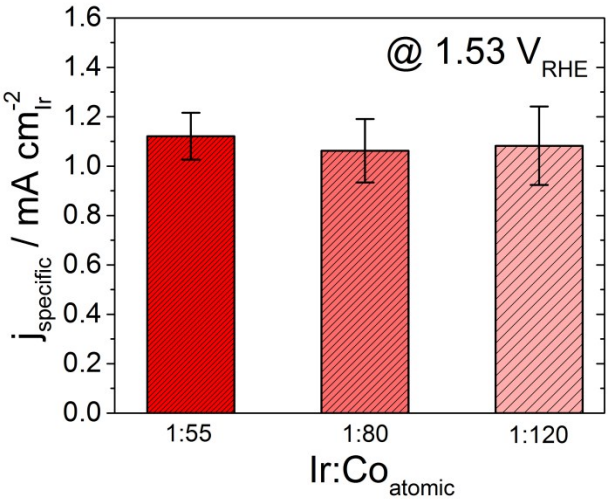

Figure S11 Specific activity for different Ir:Co atomic ratios obtained in 0.1 M $HClO_4$ with iridium loadings of 10 μg_{Ir} cm^{-2}

Accelerated durability test (AST):

To test the stability of the Ir-network catalyst, accelerated durability tests (AST) were performed by holding a potential of 1.6 V_{RHE} for 12 hours. To avoid formation of bubbles at the electrode during the AST, the electrode was constantly rotated at a speed of 3000 rpm. After each test, the electrolyte was exchanged with fresh 0.1 M $HClO_4$ electrolyte before evaluating the activity, as described above.

Previous work employing nearly identical conditions were found to produce comparable losses in single cell PEM electrolyzers with low loadings.[9] Additionally, these tests allow direct comparison between different catalysts with different loading, unlike durability tests where the geometric current density is fixed for an extended period.

Literature comparison of Ir-based OER catalysts

Table S2 Comparison of OER mass activities (j_{mass}) for IrO_x-network activity and previously reported state-of-art Ir-based OER catalysts. Values of the most frequently reported potentials of 1.51 V_{RHE}, 1.53 V_{RHE}, 1.55 V_{RHE} and 1.60 V_{RHE}. Due to insufficient stability, Ru-based and Ir supported on carbon black catalysts have not been included.

Catalyst	j_{mass} [A g^{-1}_{Ir}]				η [mV]	Loading [μg cm^{-2}]	Electrolyte	Scan rate [mV s^{-1}]	Reference
	1.51 V_{RHE}	1.53 V_{RHE}	1.55 V_{RHE}	1.60 V_{RHE}	10 mA cm^{-2}				
IrO_x-network	**313**	**817**	**1862**	**8505**	**305**	**10**	**0.1 M $HClO_4$**	**20 (LSV)**	**This work**
IrO_x-network	**254**	**670**	**1512**	**7432**	**309**	**10**	**0.1 M $HClO_4$**	**5 (CV)[f]**	**This work**
Ir-black	50	138	295	1030	-	17.8	0.1 M $HClO_4$	20 (LSV)	[9]
Ir/ATO[a]	76	177	393	-	330	20	0.5 M H_2SO_4	5 (LSV)	[7]
$IrNiO_x$[b]/ATO[a]	-	311	700	-	329	10.2	0.05 M H_2SO_4	5 (LSV)	[17]
IrNi 2d NF[c]	220	-	995	-	-	11.7	0.1 M $HClO_4$	CA[e]	[18]
IrCo NW[d]	594	1300	2327	9942	-	30.6	0.1 M $HClO_4$	20 (LSV)	[19]
IrNi NW[d]	810	1650	3353	9666	-	30.6	0.1 M $HClO_4$	20 (LSV)	[19]

[a]Antimony-doped tin oxide, [b]Core-shell nanoparticles, [c]Nanoframes, [d]Nanowires, [e]Chronoamperometry, [f]average of anodic and cathodic scan

References

1 S. Geiger, O. Kasian, A. M. Mingers, S. S. Nicley, K. Haenen, K. J. J. Mayrhofer and S. Cherevko, *ChemSusChem*, 2017, 10, 4140–4143.

2 Y. Yi, G. Weinberg, M. Prenzel, M. Greiner, S. Heumann, S. Becker and R. Schlögl, *Catal. Today*, 2017, 295, 32–40.

3 S. M. Alia, S. Pylypenko, K. C. Neyerlin, S. S. Kocha and B. S. Pivovar, *ECS Trans.*, 2015, 69, 883–892.

4 H. N. Nong, T. Reier, H.-S. Oh, M. Gliech, P. Paciok, T. H. T. Vu, D. Teschner, M. Heggen, V. Petkov, R. Schlögl, T. Jones and P. Strasser, *Nat. Catal.*, 2018, 1, 841–851.

5 Y. Garsany, I. L. Singer and K. E. Swider-Lyons, *J. Electroanal. Chem.*, 2011, 662, 396–406.

6 M. Inaba, J. Quinson and M. Arenz, *J. Power Sources*, 2017, 353, 19–27.

7 C. Massué, V. Pfeifer, X. Huang, J. Noack, A. Tarasov, S. Cap and R. Schlögl, *ChemSusChem*, 2017, 10, 1943–1957.

8 C. C. L. McCrory, S. Jung, I. M. Ferrer, S. M. Chatman, J. C. Peters and T. F. Jaramillo, *J. Am. Chem. Soc.*, 2015, 137, 4347–4357.

9 S. M. Alia, B. Rasimick, C. Ngo, K. C. Neyerlin, S. S. Kocha, S. Pylypenko, H. Xu and B. S. Pivovar, *J. Electrochem. Soc.*, 2016, 163, F3105–F3112.

10 S. M. Alia, K. E. Hurst, S. S. Kocha and B. S. Pivovar, *J. Electrochem. Soc.*, 2016, 163, F3051–F3056.

11 R. Woods, *J. Electroanal. Chem. Interfacial Electrochem.*, 1974, 49, 217–226.

12 H. Y. Hall and P. M. A. Sherwood, *J. Chem. Soc. Faraday Trans. 1 Phys. Chem. Condens. Phases*, 1984, 80, 135.

13 V. Pfeifer, T. E. Jones, J. J. Velasco Vélez, C. Massué, R. Arrigo, D. Teschner, F. Girgsdies, M. Scherzer, M. T. Greiner, J. Allan, M. Hashagen, G. Weinberg, S. Piccinin, M. Hävecker, A. Knop-Gericke and R. Schlögl, *Surf. Interface Anal.*, 2016, 48, 261–273.

14 S. J. Freakley, J. Ruiz-Esquius and D. J. Morgan, *Surf. Interface Anal.*, 2017, 49, 794–799.

15 R. Kötz, H. Neff and S. Stucki, *J. Electrochem. Soc.*, 1984, 131, 72.

16 U.S. Secretary of Commerce, NIST XPS data, https://srdata.nist.gov/xps/selEnergyType.aspx, (accessed 13 June 2019).

17 H. N. Nong, H.-S. Oh, T. Reier, E. Willinger, M.-G. Willinger, V. Petkov, D. Teschner and P. Strasser, *Angew. Chemie Int. Ed.*, 2015, 54, 2975–2979.

18 F. Godínez-Salomón, L. Albiter, S. M. Alia, B. S. Pivovar, L. E. Camacho-Forero, P. B. Balbuena, R. Mendoza-Cruz, M. J. Arellano-Jimenez and C. P. Rhodes, *ACS Catal.*, 2018, 8, 10498–10520.

19 S. M. Alia, S. Shulda, C. Ngo, S. Pylypenko and B. S. Pivovar, *ACS Catal.*, 2018, 8, 2111–2120.